

Inclusive production of neutral strange particles in 250-GeV/c π^-p interactions*

D. Bogert, R. Hanft, R. Harris, F. R. Huson, S. Kahn,[†] C. Pascaud,[‡] and W. M. Smart
Fermi National Accelerator Laboratory, Batavia, Illinois 60510

J. R. Albright, S. Hagopian, P. Hays, and J. E. Lannutti
Florida State University, Tallahassee, Florida 32306
 (Received 18 April 1977)

Neutral-strange-particle production has been studied in a 46000-picture exposure in the Fermilab 15-ft bubble chamber. Cross sections for inclusive production of K_S^0 , Λ , and $\bar{\Lambda}$ are given and compared with data at lower energies. The K_S^0 's are produced principally in the central region of rapidity with a cross section which increases with energy. The Λ 's are produced principally by proton fragmentation, whereas the $\bar{\Lambda}$'s are centrally produced. Correlations of $K_S^0\pi^+$ and $K_S^0K_S^0$ are shown to be different from those for $\pi^-\pi^+$.

This report presents results of a study of inclusive production of neutral strange particles at 250 GeV/c from the first experiment using hadrons in the Fermilab 15-ft. bubble chamber. In this chamber the detection efficiencies for K_S^0 's, Λ 's, and $\bar{\Lambda}$'s are higher than has been possible in previous experiments.

The data come from a 46 000-picture exposure of 250-GeV/c π^-p interactions. The film was scanned for all V 's which could be candidates for K^0 , Λ , or $\bar{\Lambda}$, that is, all V 's with no identified electron. The scanning efficiency for such V 's was 88%. The V 's were measured and processed through the HYDRA geometry and kinematics programs. Kinematic fits were tried to $K_S^0 \rightarrow \pi^-\pi^+$, $\Lambda \rightarrow p\pi^-$, $\bar{\Lambda} \rightarrow \bar{p}\pi^+$, and $\gamma(p_s) \rightarrow e^+e^-(p_s)$, where the last fit assumed a proton "spectator." The system efficiency to obtain some fit with at least a 1.5% χ^2 probability was about 90%.

Approximately 68% of the V 's fitted two or more hypotheses. Ambiguities involving γ 's were resolved by comparing the momentum of the electron transverse to the γ direction, p_{\perp} , with a maximum value which was taken to depend upon the momentum of the γ as follows: $p_{\perp \max} = 0.01 \text{ GeV}/c + 0.0013 p(\gamma)$ [with $p(\gamma)$ in GeV/c] for $p(\gamma) > 15 \text{ GeV}$, or $p_{\perp \max} = 0.025 \text{ GeV}/c$ for $p(\gamma) < 15 \text{ GeV}/c$. Thus V 's with an opening angle near zero (with the criteria loosened where measuring errors were larger) were assumed to be γ 's. The losses of K_S^0 , Λ , and $\bar{\Lambda}$ particles resulting from the use of these criteria are estimated to be 0.6%, 1.5%, and 2%, respectively, by comparing the p_{\perp} distributions with those predicted by assuming isotropic decay of the strange particles.

Ambiguities between K_S^0 's and Λ 's were resolved by comparing the ratio of the probabilities of the two fits to a momentum-dependent function which is proportional to the ratio of unambiguous K_S^0 's to Λ 's (this favors Λ 's of low energy and

K_S^0 's of high energy). The distribution of $\cos\theta$, where θ is the center-of-mass angle between the direction of the V and one of its decay particles, is sensitive to the resolution of these ambiguities, and is found to be reasonably flat for K_S^0 's, Λ 's, and $\bar{\Lambda}$'s. The contaminations from strange-particle ambiguities estimated from the $\cos\theta$ plots are ~4% for K_S^0 , ~5% for Λ , and ~10% for $\bar{\Lambda}$.

After resolving ambiguities, the number of events assigned to each category was 1059 K_S^0 's, 427 Λ 's, and 103 $\bar{\Lambda}$'s.

For calculating cross sections, a further cut was required to remove biases due to loss of V 's close to the primary vertex and those lost in the forward jet. This criterion was determined by studying the lifetime distributions for the K_S^0 's, Λ 's, and $\bar{\Lambda}$'s. Reasonable results were obtained after requiring a minimum length for the neutral particle of 0.75 l for K_S^0 's and 0.25 l for Λ 's and $\bar{\Lambda}$'s, where l , in each case, is the respective mean decay length in the laboratory. The final numbers of events used for cross-section calculations are given in Table I.

Inclusive cross sections were obtained by weighting each V to correct losses due to the minimum-length cut, for those which decayed outside of the fiducial volume (a sphere of radius 1.6 m), for V scanning efficiency ($93 \pm 6\%$ after correction for the minimum-length cut), and for unseen neutral decay modes. No distinction was made between Λ and Σ^0 , and the contribution from K_L^0 was not included. The resulting cross sections for inclusive production of single and double V 's are given in Table I.

Figure 1 shows the momentum dependence² of the inclusive cross sections for K_S^0 , Λ , and $\bar{\Lambda}$. The K_S^0 and $\bar{\Lambda}$ cross sections increase with momentum while Λ cross section is approximately constant above 20 GeV/c.

The center-of-mass rapidity distributions for

TABLE I. Inclusive cross sections.

Reaction	Cross section (mb)	No. of events
$\pi^-p \rightarrow K_S^0 + X$	3.98 ± 0.5	624
$\rightarrow \Lambda + X$	1.47 ± 0.2	362
$\rightarrow \bar{\Lambda} + X$	0.41 ± 0.09	82
$\rightarrow K_S^0 K_S^0 + X$	0.62 ± 0.2	30
$\rightarrow K_S^0 \Lambda + X$	0.41 ± 0.1	30
$\rightarrow K_S^0 \bar{\Lambda} + X$	0.13 ± 0.06	7
$\rightarrow \Lambda \bar{\Lambda} + X$	0.15 ± 0.06	9
$\rightarrow \Lambda \Lambda + X$	0.04 ± 0.02	5
$\rightarrow (\geq 3V) + X$	(see footnote a)	

^aThere were 12 events with 3 observed V 's and one $4V$ event. After applying the bias cut, only 3 of the $3V$ events remained. Events observed were: four $K_S^0 K_S^0 K_S^0$, six $K_S^0 K_S^0 \Lambda$, two $K_S^0 \Lambda \bar{\Lambda}$, and one $K_S^0 K_S^0 K_S^0 \Lambda$.

K_S^0 's, Λ 's, and $\bar{\Lambda}$'s are shown in Fig. 2. For the K_S^0 's, the rapidity distribution shown in Fig. 2(a) is consistent with the existence of a plateau of approximately two units symmetrically centered at zero. For comparison, the $d\sigma/dy$ distribution at 100 GeV/c,² which is available only for $y < 0$, is also shown. It appears that the values in the central region of rapidity are approximately equal at 100 and 250 GeV/c.

Above 100 GeV/c, most models which include central-region production predict a $\ln s$ or $(\ln s)^2$ increase in cross section. There is an expected $\ln s$ increase due to the increase in the width of the rapidity plateau and another factor of $\ln s$ if the plateau height increases like that seen for pions.¹ Although the rising cross section for K_S^0 's and the central rapidity plateau indicate central production, data on $\sigma(K_S^0)$ as they stand are insufficient to allow us to choose between the two alternatives of $\ln s$ or $(\ln s)^2$ dependence for $\sigma(K_S^0)$.

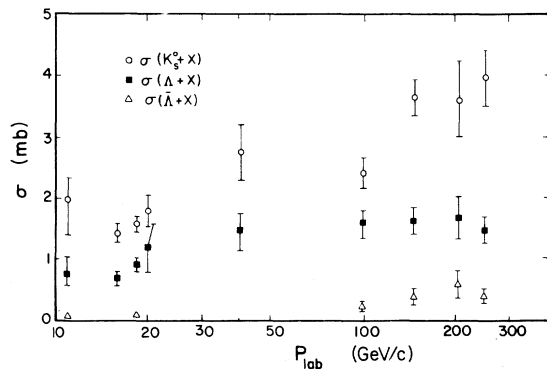


FIG. 1. Inclusive production cross sections for K_S^0 , Λ , and $\bar{\Lambda}$ as a function of laboratory momentum. Data for other momenta obtained as given in Ref. 2.

The $d\sigma/dy$ distribution for Λ 's in Fig. 2(b) shows a maximum in the negative- y region. This is as expected if most of the production is due to fragmentation of the target proton.³ However, there is significant production of Λ 's near $y=0$. This is to be compared with $d\sigma/dy$ for $\bar{\Lambda}$'s, in Fig. 2(c), which is approximately equal to $d\sigma/dy$ for Λ 's at $y=0$ and essentially symmetric about $y=0$. However, this does not necessarily imply the dominance of $\Lambda\bar{\Lambda}$ -pair production in this region since, as shown in Table I, $\bar{\Lambda}$'s are also produced with K_S^0 's.

The production of these particles can be further clarified by examining the relation between rapidities of pairs of strange particles. Figure 3 shows scatter plots of the rapidity of one V versus that of the other V for the pairs $K_S^0 K_S^0$, $K_S^0 \Lambda$, $K_S^0 \bar{\Lambda}$, and $\Lambda \bar{\Lambda}$. To improve statistics the bias cuts used

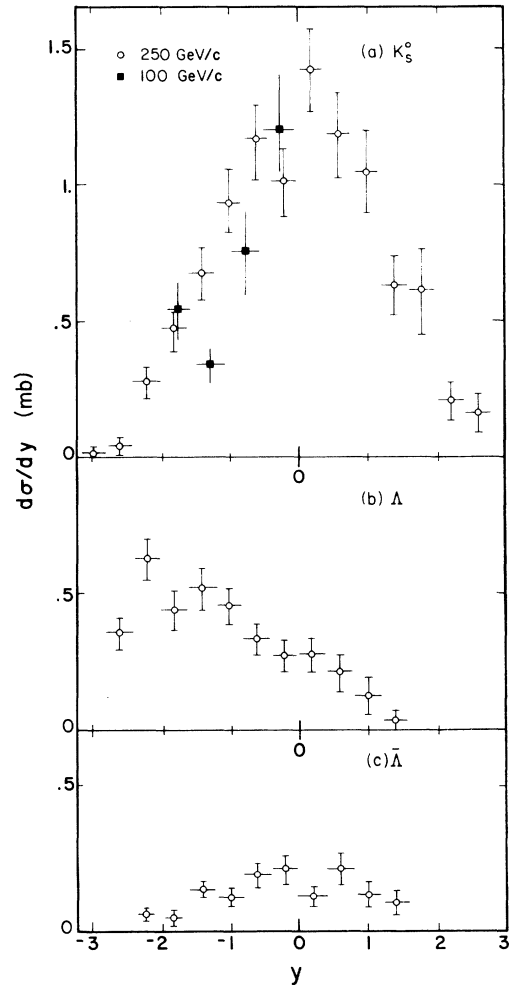


FIG. 2. $d\sigma/dy$ center-of-mass rapidity distributions for (a) K_S^0 's, (b) Λ 's, (c) $\bar{\Lambda}$. For $d\sigma(K_S^0)/dy$, the distribution for 100 GeV/c for $y < 0$ is also given for comparison.

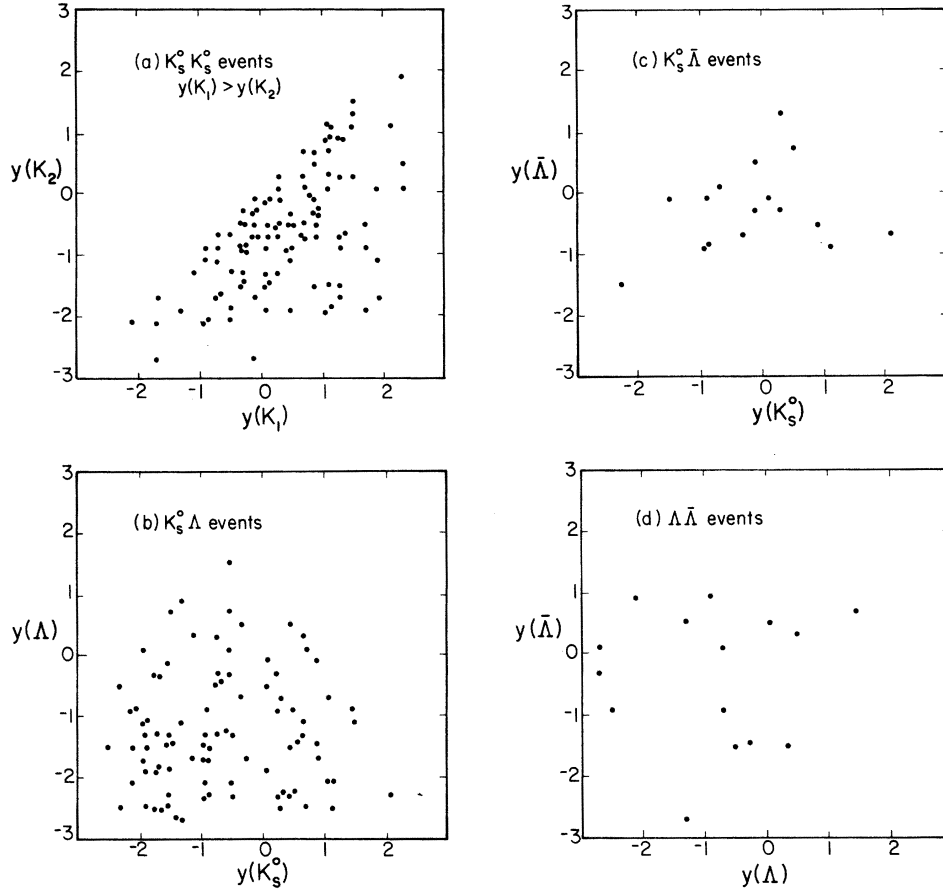


FIG. 3. Scatter plots of the rapidity of V_1 versus the rapidity of V_2 in double- V events: (a) $K_S^0 K_S^0$ [plotted with $y(K_1) > y(K_2)$], (b) $K_S^0 \Lambda$, (c) $K_S^0 \bar{\Lambda}$, and (d) $\Lambda \bar{\Lambda}$.

in the other figures of the paper have been ignored here. The $K_S^0 K_S^0$ and the $K_S^0 \bar{\Lambda}$ plots are denser in the center indicating strong central pair production. The $K_S^0 \Lambda$ plot shows roughly one-third central production ($y_\Lambda > -1.0$), and a significant fraction of events with both y_Λ and $y_{K_S^0}$ in the proton fragmentation region. The $\Lambda \bar{\Lambda}$ plot shows mostly central-region pairs, but also has events with large negative- Λ rapidity.

To investigate scaling, the invariant cross sections $F_1(x)$ and $F_2(p_1^2)$ are shown in Fig. 4, where

$$F_1(x) = \frac{2}{\pi\sqrt{s}} \int E^* \frac{d\sigma^2}{dx dp_1^2} dp_1^2,$$

$$F_2(p_1^2) = \frac{2}{\pi\sqrt{s}} \int E^* \frac{d\sigma^2}{dx dp_1^2} dx.$$

The $F_1(x)$ distributions are compared with data at 18.5 GeV/c (Ref. 2) in Figs. 4(a), 4(b), and 4(c). The distributions for K_S^0 and $\bar{\Lambda}$ do not scale; the K_S^0 distributions differ in shape, while the $\bar{\Lambda}$ distributions differ in magnitude. Although the Λ distribution does appear to scale, this may be for-

titious since a significant fraction of the cross section at $x=0$ can be attributed to $\Lambda \bar{\Lambda}$ production at 250 GeV/c, whereas this is certainly not true at 18.5 GeV/c.

The $F_2(p_1^2)$ distributions in Fig. 4(d) have been fitted to simple exponentials over the region $0 < p_1^2 < 1$ (GeV/c)², yielding slopes of (3.20 ± 0.3) (GeV/c)⁻², (3.0 ± 0.3) (GeV/c)⁻², and (2.5 ± 0.6) (GeV/c)⁻² for K_S^0 's, Λ 's, and $\bar{\Lambda}$'s, respectively. The slope for Λ 's is slightly larger than that for $\bar{\Lambda}$'s, as might be expected, since Λ production has been shown to be primarily via fragmentation, which results in smaller average p_1^2 . There is some evidence in Fig. 4(d) that the Λ distribution is steeper at small p_1^2 than at large p_1^2 .

The correlation between neutral-strange-particle production and charged π 's can be seen in the dependence of the average number of V 's, $\langle n_v \rangle$, with charged multiplicity, as shown in Table II and Fig. 5. The $\langle n_{K_S^0} \rangle$ distribution seems to exhibit a distinct rise with multiplicity similar to that seen for π^0 production.¹ This effect is not as

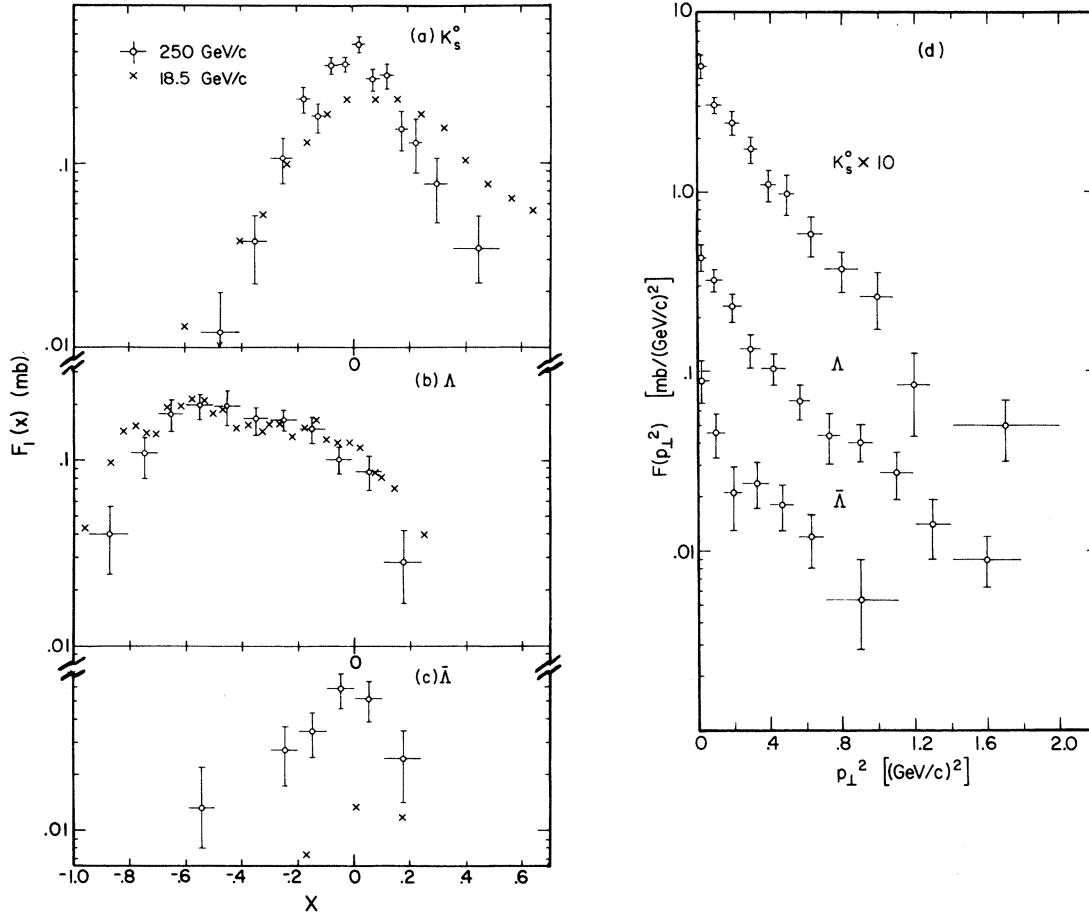


FIG. 4. Invariant function $F_1(x)$ is given for (a) K_S^0 's, (b) Λ 's, (c) $\bar{\Lambda}$'s. For comparison, data for 18.5 GeV/c is also given with the $F_1(x)$ distributions. (d) Gives the invariant function $F_2(p_1^2)$ for K_S^0 's, Λ 's, and $\bar{\Lambda}$'s. The K^0 data in (d) have been multiplied by a factor of 10 to separate it from the Λ data.

TABLE II. Multiplicity dependence of strange-particle production.

No. of prongs	K_S^0			Λ			$\bar{\Lambda}$		
	No. of K_S^0 's	σ (mb)	$\langle n_{K_S^0} \rangle$	No. of Λ 's	σ (mb)	$\langle n_{\Lambda} \rangle$	No. of $\bar{\Lambda}$'s	σ (mb)	$\langle n_{\bar{\Lambda}} \rangle$
0	2	0.11 ± 0.008	0.85 ± 0.7	2	0.007 ± 0.005	0.54 ± 0.4	0
2	17	0.11 ± 0.03	0.06 ± 0.02	13	0.05 ± 0.01	0.024 ± 0.008	2	0.01 ± 0.01	0.007 ± 0.006
4	47	0.31 ± 0.05	0.10 ± 0.02	39	0.14 ± 0.02	0.045 ± 0.007	5	0.02 ± 0.01	0.008 ± 0.004
6	106	0.66 ± 0.07	0.17 ± 0.02	71	0.28 ± 0.03	0.071 ± 0.009	19	0.09 ± 0.02	0.025 ± 0.006
8	118	0.76 ± 0.07	0.20 ± 0.02	70	0.30 ± 0.04	0.08 ± 0.01	16	0.08 ± 0.02	0.019 ± 0.005
10	100	0.64 ± 0.07	0.20 ± 0.02	62	0.26 ± 0.04	0.08 ± 0.01	20	0.11 ± 0.03	0.033 ± 0.008
12	102	0.66 ± 0.07	0.29 ± 0.03	46	0.19 ± 0.03	0.08 ± 0.01	7	0.03 ± 0.01	0.013 ± 0.005
14	66	0.39 ± 0.05	0.28 ± 0.04	28	0.12 ± 0.02	0.08 ± 0.02	5	0.03 ± 0.01	0.019 ± 0.009
16	27	0.17 ± 0.03	0.23 ± 0.05	12	0.05 ± 0.01	0.06 ± 0.02	2	0.007 ± 0.005	0.010 ± 0.007
18	22	0.12 ± 0.03	0.38 ± 0.07	5	0.019 ± 0.009	0.05 ± 0.02	2	0.01 ± 0.01	0.04 ± 0.03
20	10	0.06 ± 0.02	0.30 ± 0.1	9	0.04 ± 0.01	0.19 ± 0.07	2	0.01 ± 0.01	0.07 ± 0.05
>20	7	0.05 ± 0.02	0.40 ± 0.18	5	0.03 ± 0.01	0.30 ± 0.14	2	0.008 ± 0.005	0.30 ± 0.2
Total	624	3.98 ± 0.5	0.19 ± 0.02	362	1.47 ± 0.2	0.070 ± 0.008	82	0.41 ± 0.09	0.020 ± 0.003

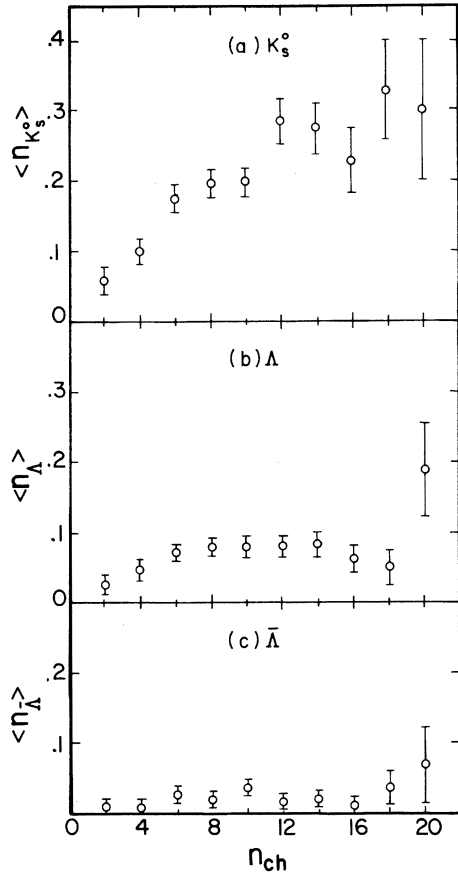


FIG. 5. Average number of K_S^0 's, Λ 's, and $\bar{\Lambda}$'s as a function of the number of charged prongs.

obvious in lower-energy πp experiments,⁴ which are consistent with $\langle n_{K_S^0} \rangle$ being constant with multiplicity. The $\langle n_{\Lambda} \rangle$ distribution is consistent with being constant with respect to multiplicity above $n=4$, as would be expected since target fragmentation dominates Λ production.

To study the differences in correlations between π 's and K 's, we have calculated the correlation function $R(\Delta y)$, where $\Delta y = y_2 - y_1$ and

$$R(y_1, y_2) = \frac{\rho_{12}(y_1, y_2)}{\rho_1(y_1)\rho_2(y_2)} - 1,$$

$$\rho_{12} = \frac{1}{\sigma_{inel}} \frac{d^2\sigma}{dy_1 dy_2},$$

$$\rho_1 = \frac{1}{\sigma_{inel}} \frac{d\sigma}{dy_1},$$

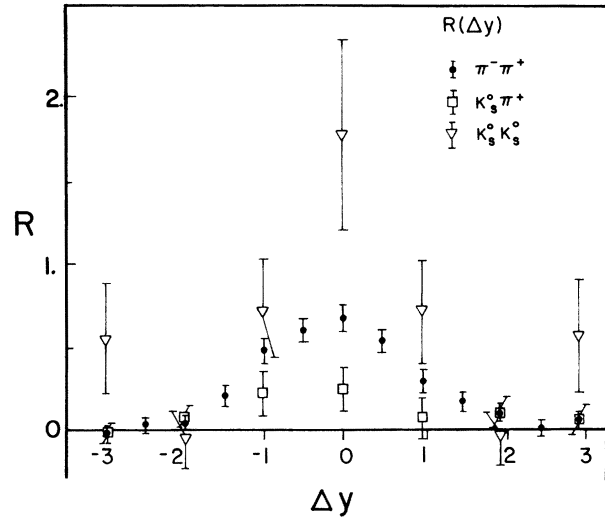


FIG. 6. Correlation function $R(\Delta y)$, defined in the text, for particle pairs $\pi^+ \pi^-$, $K_S^0 \pi^+$, and $K_S^0 K_S^0$.

in which ρ_{12} , ρ_2 , and ρ_1 are the double and single rapidity densities. $R(\Delta y)$ was obtained by integrating $R(y_1, y_2)$ with respect to y_1 and y_2 over the region $-2 < y_2 < 2$, $-2 < y_1 < 2$. This function is shown for $\pi^- \pi^+$, $K_S^0 \pi^+$, and $K_S^0 K_S^0$ pairs in Fig. 6. Here π includes all charged particles except identified protons. The $R(\pi^- \pi^+)$ distribution is in good agreement with an experiment at 205 GeV/c which has better statistics.⁵ The $K_S^0 \pi^+$ pairs show smaller correlation than $\pi^- \pi^+$, while the $K_S^0 K_S^0$ pairs show a significantly larger correlation at $\Delta y = 0$.

In conclusion, we have shown that K_S^0 's are produced predominantly in the central region, with a cross section which increases with energy. The $\langle n_{K_S^0} \rangle$ exhibits an increase with multiplicity and $K_S^0 K_S^0$ pairs show a strong correlation at $\Delta y = 0$. All this is qualitatively similar to what is known about the production of charged and neutral π 's. The production of Λ 's is mostly associated with the fragmentation of the proton, whereas the $\bar{\Lambda}$'s are centrally produced.

We appreciate the support given to us by the Fermilab beam and bubble chamber crews during the pioneering 15-ft.-bubble-chamber run. We are grateful to the scanning staffs at both laboratories. We would like to thank R. Bates, M. Harrison, and M. Sokoloff for help in the analysis, and J. F. Owens for useful comments.

*Work supported in part by the U. S. Energy Research and Development Administration.

†Present address: Brookhaven National Laboratory, Upton, New York.

‡Present address: Laboratoire de l'Accélérateur linéaire, Orsay, France.

¹J. Whitmore, Phys. Rep. **27C**, 187 (1976).

²11.5 GeV/c: T. Ferbel and H. Taft, Nuovo Cimento

28, 1214 (1963); 16 GeV/c: J. Bartke *et al.*, *ibid.* 24, 376 (1962); 18.5 GeV/c: P. H. Stuntebeck *et al.*, Phys. Rev. D 9, 608 (1974); 20 GeV/c: E. Balea *et al.*, Rev. Roum. Phys. 15, 587 (1970); 40 GeV/c: E. Balea *et al.*, Nucl. Phys. B79, 57 (1974); 100 GeV/c: E. L. Berger *et al.*, CERN Report No. CERN/D. PhII/PHYS 74-27, 1974 (unpublished); 147 GeV/c: T. Watts, private communication; 205 GeV/c: D. Ljung *et al.*, Phys. Rev. D 15, 3163 (1977).

²It is also interesting that J. F. Owens has been able to predict the magnitude and momentum dependence of $\sigma(\Lambda)$ covered in Fig. 1 using a pure fragmentation model with no free parameters (private communication).

⁴S. Kahn, in *Particles and Fields—1975*, proceedings of the meeting of the Division of Particles and Fields of the APS, Seattle, edited by H. J. Lubatti and P. M. Mockett (Univ. of Washington, Seattle, 1975), p. 292.

⁵N. N. Biswas *et al.*, Phys. Rev. Lett. 35, 1059 (1975).